Journal of Power Sources 196 (2011) 3039–3047

Contents lists available at ScienceDirect

Journal of Power Sources

journal homepage: www.elsevier.com/locate/jpowsour

Synthesis and properties of novel sulfonated polybenzimidazoles from disodium 4,6-bis(4-carboxyphenoxy)benzene-1,3-disulfonate

Li Sheng, Hongjie Xu*, Xiaoxia Guo, Jianhua Fang*, Liang Fang, Jie Yin

School of Chemistry and Chemical Engineering, State Key Laboratory of Metal Matrix Composite Materials, Shanghai Jiao Tong University, 800 Dongchuan Road, Shanghai 200240, China

ARTICLE INFO

Article history:
Received 18 October 2010
Received in revised form
12 November 2010
Accepted 22 November 2010
Available online 27 November 2010

Keywords:
Sulfonated polybenzimidazole
Membrane
Phosphoric acid doping
Proton conductivity
Fuel cell performance

ABSTRACT

A series of sulfonated polybenzimidazoles (SPBIs) with varied ion exchange capacities (IECs) have been synthesized by random condensation copolymerization of a new sulfonated dicarboxylic acid monomer 4,6-bis(4-carboxyphenoxy)benzene-1,3-disulfonate (BCPOBDS-Na), 4,4′-dicarboxydiphenyl ether (DCDPE) and 3,3′-diaminobenzidine (DAB) in Eaton's reagent at 140 °C. Most of the SPBIs show good solubility in polar aprotic organic solvents such as dimethylsulfoxide (DMSO) and N,N-dimethylacetamide (DMAc). Thermogravimetric analysis (TGA) reveals that the SPBIs have excellent thermal stability (desulfonation temperatures (on-set) > 370 °C). The SPBI membranes show good mechanical properties of which tensile strength, elongation at break, and storage modulus are in the range of 89–96 MPa, 12–42%, and 2.4–3.1 GPa, respectively. Moreover, the SPBI membranes exhibit phosphoric acid (PA) uptake in the range of 180–240% (w/w) in 85 wt% PA at 50 °C, while high mechanical properties (13–20 MPa) are maintained. The SPBI membrane with 240% (w/w) PA uptake displays fairly high proton conductivity (37.3 mS cm^{-1}) at 0% relative humidity at 170 °C. The fuel cell fabricated with the PA-doped SPBI membrane (PA uptake = 240% (w/w)) displays good performance with the highest output power density of 0.58 W cm^{-2} at 170 °C with hydrogen–oxygen gases under ambient pressure without external humidification.

1. Introduction

Polymer electrolyte membrane fuel cells (PEMFCs) are one of the most promising power sources for both mobile and stationary applications [1,2]. A proton exchange membrane (PEM) is one of the key components of a PEMFC system, which functions as the anode/cathode separator as well as the medium for proton transport from the anode to the cathode. Up to date, the state-of-the-art PEMs are sulfonated perfluoropolymers, typically, Dupont's Nafion because of its excellent chemical and electrochemical stability and high proton conductivity. However, some disadvantages such as high cost, high fuel crossover and low operating temperatures (<100 °C) seriously limited their industrial application. In the past decade, many efforts have been made to develop cost-effective and high performance non-fluorinated membranes as alternatives such as sulfonated polysulfone (SPSF) [3–6], sulfonated poly(ether ether ketone)s (SPEEK) [7–10], sulfonated polyphenylene [7,11,12], sulfonated polyimides (SPIs) [13–16] and sulfonated polybenzimidazoles (SPBIs) [17–27].

Aromatic polybenzimidazoles (PBIs), known for their excellent thermal and thermoxidative stability, high mechanical strength and storage modulus, and outstanding chemical resistance, have found important industrial applications. The cross-linked SPBI membranes have been reported to have excellent radical oxidative stability which is very favorable for improving fuel cell lifetime [26]. Up to date, many kinds of SPBIs have been synthesized and studied for possible use in fuel cells. However, compared with common sulfonated polymer membranes containing no basic units in their chemical structures SPBIs generally show rather low proton conductivity because the proton transport becomes relatively difficult resulting from the strong acid–base interactions between the sulfonic acid groups and basic imidazole rings [24]. One mole imidazole ring can react with one mole sulfonic acid group to form ionic cross-linking. As the mole number of sulfonic acid groups is less than that of imidazole ring, the proton conductivity is generally at the level of 10^{-4}–10^{-3} S cm^{-1} even at 100% relative humidity which is too low to meet the lowest requirement (10^{-2} S cm^{-1}) for practical use [24]. On the other hand, PBIs can be doped with a number of acids such as sulfuric acid and phosphoric acid (PA). It has been reported that the PA-doped PBIs displayed high proton conductivities even under anhydrous conditions which makes them very suitable for use in medium temperature (120–200 °C) fuel cells [28–37]. The proton conductivity is mainly determined by

* Corresponding authors. Tel.: +86 21 54747504; fax: +86 21 54741297.
E-mail addresses: hjxu@sjtu.edu.cn (H. Xu), jhfang@sjtu.edu.cn (J. Fang).

0378-7753/$ – see front matter © 2010 Elsevier B.V. All rights reserved.
doi:10.1016/j.jpowsour.2010.11.121

the PA-doping level, and the higher doping level, the higher proton conductivity. Recently Gomez-Romero et al. reported an interesting phenomenon that the SPBI derived from 5-sulfoisophthalic acid mono-sodium salt and 1,2,4,5-tetraaminobenzene displayed higher proton conductivity than the non-sulfonated PBIs at the same doping level (number of PA molecules per imidazole ring). This should be favorable for achieving high fuel cell performance. However, the structure–property relationship of SPBIs and in particular, the fuel cell performance have far less been investigated yet. In this study, a novel sulfonated dicarboxylic acid monomer, disodium 4,6-bis(4-carboxyphenoxy)benzene-1,3-disulfonate (BCPOBDS-Na), was synthesized via multistep reactions and a series of SPBIs with varied ion exchange capacities (IECs) were prepared via random copolymerization of BCPOBDS-Na, 4,4′-dicarboxydiphenyl ether (DCDPE) and 3,3′-diaminobenzidine (DAB) in Eaton's reagent. The thermal stability, mechanical properties, radical oxidative stability, PA-doping, proton conductivity and fuel cell performance of the SPBI membranes were also investigated.

2. Experimental

2.1. Materials

3,3′-Diaminobenzidine (DAB), 4-fluorobenzonitrile, 1,3-dihydroxybenzene and 4,4′-dicarboxydiphenyl ether (DCDPE) were purchased from Acros. Phosphorus pentoxide, methanesulfonic acid, dimethylsulfoxide (DMSO), 1-methylpyrrolidone (NMP), N,N-dimethylformamide (DMF) and N,N-dimethylacetamide (DMAc) were purchased from Sinopharm Chemical Reagent Co., Ltd. (SCRC). Eaton's reagent was prepared by dissolving phosphorus pentoxide in methanesulfonic acid at a weight ratio of 1:10. DMSO, NMP, DMAc and DMF were dried over 4A molecular sieves prior to use. Other materials were used as received.

2.2. Synthesis of 1,3-bis(4-cyanophenoxy)benzene (mBCNPOB)

To a 150 mL dry three-necked flask equipped with a nitrogen inlet and an outlet, a dropping funnel, a Dean-Stark trap and a condenser were added 5.51 g (50 mmol) of 1,3-dihydroxybenzene, 13.81 g (100 mmol) of K_2CO_3 and 60 mL DMAc. The reaction mixture was magnetically stirred at room temperature for 2 h and then heated at 140 °C for 5 h. 20 mL toluene in the dropping funnel was added to remove any water by forming toluene–water azeotrope which was collected in the Dean-Stark trap. The reaction mixture was allowed to cool to room temperature and then 12.11 g (100 mmol) of 4-fluorobenzonitrile was introduced, and the mixture was further heated at 160 °C for 24 h. After cooling to room temperature, the reaction mixture was poured into deionized water with stirring. The resulting brown precipitate was filtered off, washed with deionized water and dried at 70 °C for 20 h in vacuum. 14.51 g (yield: 93%) of brownish product was obtained, mp (by differential scanning calorimetry (DSC)): 122 °C. ^{1}H NMR (DMSO–d_6, ppm): 6.79 (s, 1H), 6.92 (d, 2H), 7.05 (d, 4H), 7.42 (t, 1H), 7.64 (d, 4H). ^{13}C NMR (DMSO–d_6, ppm): 106.24, 112.81, 117.18, 119.12, 119.31, 132.56, 135.38, 156.69 and 161.20.

2.3. Synthesis of 1,3-bis(4-carboxyphenoxy)benzene (mBCPOB)

To a 500 mL dry three-necked flask equipped with a nitrogen inlet and an outlet and a condenser were added 8.11 g (26 mmol) of *m*BCNPOB, 7.28 g (130 mmol) of KOH and 195 mL glycol. The reaction mixture was magnetically stirred and heated at 180 °C for 24 h followed by vacuum distillation to remove the solvent glycol. The solid product was dissolved in deionized water and then acidified with concentrated hydrochloric acid till the pH = 1. The white precipitate was collected by filtration, thoroughly washed with deionized water and dried in vacuum at 120 °C for 20 h. 7.55 g (yield: 83%) of white product was obtained, mp (by DSC): 300 °C. ^{1}H NMR (DMSO–d_6, ppm): 6.85 (s, 1H), 6.94 (d, 2H), 7.08 (d, 4H), 7.48 (t, 1H), 7.94 (d, 4H), 12.80 (s, 1H). ^{13}C NMR (DMSO–d_6, ppm): 112.01, 116.24, 118.32, 126.38, 132.29, 132.27, 157.34, 161.01 and 167.35.

2.4. Synthesis of disodium 4,6-bis(4-carboxyphenoxy) benzene-1,3-disulfonate (BCPOBDS-Na)

To a 150 mL dry flask were added 7.00 g (20 mmol) *m*BCPOB and 80 mL concentrated sulfuric acid. The reaction mixture was magnetically stirred and heated at 80 °C for 24 h. After cooling to room temperature, the mixture was carefully poured into 300 g crushed ice, and then 62 g of sodium chloride was added to salt out the product. The resulting precipitate was filtered off, washed with saturated sodium chloride solution and dried at 100 °C for 20 h in vacuum. The crude product was added to 200 mL DMSO and the mixture was magnetically stirred at room temperature for 2 h. The insoluble part was filtered off and the filtrate was distilled under reduced pressure. The solid product was thoroughly washed with acetone and then dried at 120 °C for 20 h in vacuum. 7.09 g (yield: 64%) white product was obtained. MS: m/z = 553.0 ($M-H^+$), 531.0 ($M-Na^+$), 418.9 ($M-2Na^+ -2COO\cdot$).

2.5. Preparation of sulfonated copolybenzimidazoles (SPBI-xy, x and y refer to the molar ratio of BCPOBDS-Na to DCDPE)

A typical procedure is described as follows using the copolymer SPBI-11 as an example.

To a 150 mL dry three-necked flask were added 0.8561 g (4 mmol) DAB, 0.5162 g (2 mmol) DCDPE, 1.1088 g (2 mmol) BCPOBDS-Na and 20 mL Eaton's reagent under nitrogen flow. The reaction mixture was magnetically stirred and heated at 80 °C for 2 h and 140 °C for 45 min. After cooling to ~80 °C, the highly viscous solution mixture was poured into ice water with stirring. The resulting yellowish fiber-like polymer was filtered off and soaked in 5 wt% $NaHCO_3$ solution at room temperature for 48 h. The solid polymer was collected by filtration, thoroughly washed with deionized water and dried at 120 °C for 24 h under vacuum.

2.6. Membrane formation and proton exchange

The prepared SPBIs in their sodium salt form were dissolved in DMSO to give 2–4% (w/v) solutions. The solutions were cast onto glass plates and dried at 80 °C for 20 h in an air oven. The as-cast membranes were peeled off and subsequently immersed into hot methanol for 5 h to remove any residual solvent.

Proton exchange treatment was performed by immersing the SPBI membranes in 1 M sulfuric acid solution at 60 °C for two days. The membranes were taken out, thoroughly rinsed with deionized water till the rinsed water became neutral, and dried in a vacuum oven at 120 °C for 20 h.

2.7. Measurements

FT-IR spectra were recorded on a Perkin-Elmer Paragon 1000PC spectrometer. ^{1}H NMR and ^{13}C NMR spectra were recorded on a Varian Mercury Plus 400 MHz instrument. Mass spectrum (MS) were recorded with an Agilent 1100 LC/MSD instrument. Reduced viscosity (η) was measured in DMSO at a polymer concentration of 0.5 g dL^{-1} with an Ubbelohde viscometer at 30 °C. Differential scanning calorimetry (DSC) was measured in N_2 on a DSC 6200 instrument at a heating rate of 10 °C min^{-1} from room temperature to 400 °C. Thermogravimetric analysis (TGA) was performed

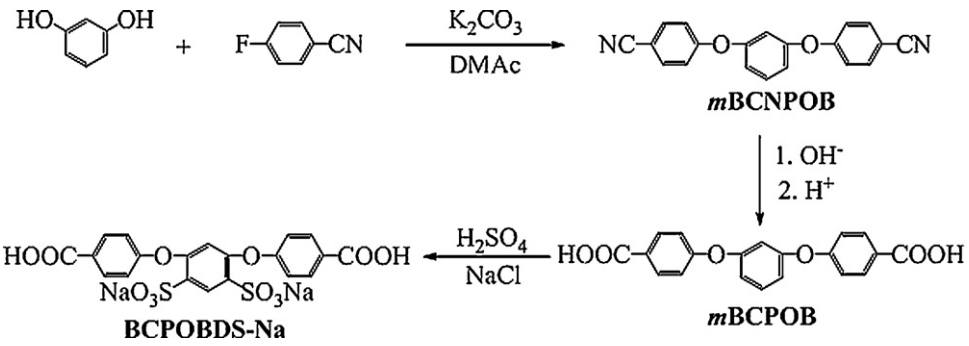

Scheme 1. Synthesis of the sulfonated dicarboxylic acid monomer BCPOBDS-Na.

in air with a TGA2050 instrument. Prior to measurement, all the samples were preheated at 150 °C for half an hour to remove the absorbed moisture. Subsequently the samples were cooled to 50 °C and then reheated to 800 °C at a heating rate of 10 °C min^{-1}. Tensile measurements were carried out with an Instron 4456 instrument at room temperature and 40% relative humidity at a crosshead speed of 5 mm min^{-1}. For each kind of membrane, three samples were used for the measurements and the tensile stress and the elongation at break was estimated by the averaged values of the three samples. Dynamic mechanical analysis (DMA) was measured on a Q800 DMA apparatus (TA Instruments, USA) in tension mode under nitrogen atmosphere at a frequency of 1.0 Hz in temperature range of 50–400 °C at a heating rate of 10 °C min^{-1}. The samples were 30 mm long, 8 mm wide and 30–40 μm thick.

Ion exchange capacity (IEC) was measured by titration method. The samples were immersed in 1.0 M NaCl solution at 40 °C for three days. After that, the samples were not taken out and the NaCl solution was directly titrated with 0.01 M NaOH using phenolphthalein as pH indicator.

The radical oxidation stability of the membranes was determined by Fenton's test. The completely dried samples were soaked in the Fenton's reagent (3% H_2O_2 containing 3 ppm $FeSO_4$) at 80 °C for 12 h. The remaining weight (RW) of the samples after Fenton's test was used to evaluate the radical oxidation stability of the membranes.

Phosphoric acid uptake (S_{PA}) of the SPBI membranes was measured by immersing the dry membranes in 85% phosphoric acid solution at 50 °C for four days. Then the membranes were taken out, wiped with tissue paper, and dried at 110 °C for 24 h in vacuum. S_{PA} was calculated according to the following equation:

$$S_{PA} = \frac{W_1 - W_0}{W_0} \times 100 \quad (1)$$

where W_0 and W_1 refer to the weight of the dry undoped membrane and the dry doped membrane, respectively.

Proton conductivity was measured using a two-probe electrochemical impedance spectroscopy technique over the frequency range from 100 to 100 kHz. A sheet of PA-doped membrane and a pair of platinum electrode was set in a Teflon cell. The cell was placed in a thermo-controlled chamber, which had an inlet and an outlet for continuous nitrogen flow. Before starting the conductivity measurement, the chamber was heated at 150 °C for one day to remove any water vapor so that the relative humidity could reach 0%. After that, the temperatures of chamber was set at desired values and kept constant for 1 h at each point. The resistance value was determined from high-frequency intercept of the impedance with the real axis. Proton conductivity was calculated from the following equation:

$$\sigma = \frac{d}{twR} \quad (2)$$

where d is the distance between the two electrodes, t and w are the thickness and width of the membrane, and R is the resistance measured.

2.8. Membrane electrode assembly (MEA) fabrication and fuel cell test conditions

The 40 wt% Pt/C (Johnson Matthey) was homogeneously dispersed in 4 wt% PBI solution in DMAc by ultrasonic treatment. The resulting catalyst ink was sprayed onto carbon cloth-based gas diffusion layers (LT 1200-W, 370 μm thick, 27 wt% PTFE, BASF fuel cell) with an airbrush followed by drying at 190 °C for 3 h in vacuum to remove the residual solvent (DMAc). The Pt loading was controlled at 0.5 mg cm^{-2} and the weight ratio of Pt/C to PBI was 19:1. The prepared gas diffusion electrodes were immersed in a 15 wt% H_3PO_4/ethanol solution for 10 min at room temperature and then they were taken out and dried at 60 °C for 1 h. The gas diffusion electrodes thus obtained were used as both the anode and the cathode. The MEA was prepared by hot pressing an electrode/membrane/electrode sandwich at 150 °C at 0.13 MPa for 10 min. The MEA with an active area of 5 cm^2 was assembled into a single cell testing fixture (FC05-MP, ElectroChem). Gases were fed to the single cell at a flow rate of 100 mL min^{-1} for H_2, 300 mL min^{-1} for O_2 and 1000 mL min^{-1} for air without any external humidification. All the performance data were collected under atmosphere pressure without back pressure detected. Current–voltage curves were measured with a DC electronic load (IT8514F) and recorded by the constant current mode at a scan rate of 400 mA min^{-1}.

Electrochemical impedance spectroscopy (EIS) was performed at the open circuit voltage (OCV). The frequency was in the range from 100 kHz to 100 MHz and the potential amplitude was 10 mV. Data were collected using a computer-controlled CHI 604B potentiostat (Chenhua, Shanghai).

3. Results and discussion

3.1. Synthesis of BCPOBDS-Na

As shown in Scheme 1, a novel sulfonated dicarboxylic acid monomer, BCPOBDS-Na, was synthesized via three-step reactions. In the first step, 4-fluorobenzonitrile reacted with 1,3-dihydroxybenzene to form the intermediate product *m*BCNPOB at a high yield of 93%. Next, *m*BCNPOB was hydrolyzed under basic condition in glycol to give the dicarboxylic acid product *m*BCPOB at a yield of 83%. Finally, *m*BCPOB was sulfonated to produce the sulfonated dicarboxylic acid monomer, BCPOBDS-Na, using 95% sulfuric acid as the sulfonating reagent. The chemical structures of the synthesized sulfonated dicarboxylic acid monomer as well as the intermediate products were characterized by FT-IR, ^{1}H NMR and ^{13}C NMR spectra. Fig. 1 shows the FT-IR spectra of *m*BCNPOB, *m*BCPOB and BCPOBDS-Na. In Fig. 1(a), the absorption band at

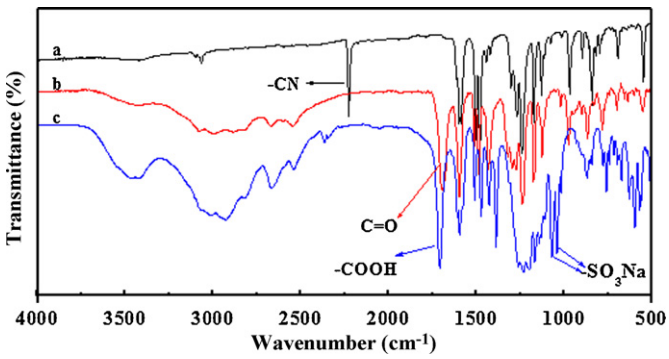

Fig. 1. FT-IR spectra of (a) *m*BCNPOB, (b) *m*BCPOB and (c) BCPOBDS-Na.

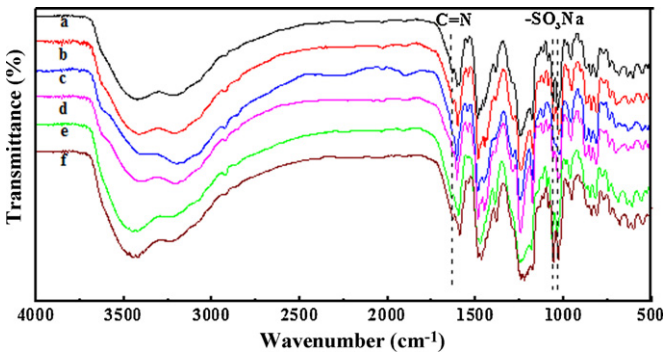

Fig. 4. FT-IR spectra of the synthesized polymers: (a) SPBI-11, (b) SPBI-12, (c) SPBI-13, (d) SPBI-14, (e) SPBI-21 and (f) SPBI-31.

2230 cm^{-1} is assigned to –C≡N stretching vibration of *m*BCNPOB. This band completely disappeared in Fig. 1(b) and a new absorption band at 1694 cm^{-1} which is attributed to the carboxyl carbonyl groups appeared. This indicates that the –C≡N groups have been completely hydrolyzed to carboxyl groups. In Fig. 1(c), the absorption bands at 1072 and 1034 cm^{-1} are assigned to the symmetric and asymmetric stretching of the sulfonic acid groups indicating that success of the sulfonation reaction. The extremely broad absorption bands in the range of 3500–2500 cm^{-1} in Fig. 1(b) and (c) are the characteristic bands of the hydroxyl groups of carboxyl or sulfonic acid groups and the water absorbed in the samples. The ^{1}H NMR and ^{13}C NMR spectra of BCPOBDS-Na are shown in Figs. 2 and 3, respectively. The peak assignments are just consistent with the chemical structure indicating that BCPOBDS-Na has been successfully synthesized.

3.2. Synthesis, solubility and viscosity of SPBIs

A series of sulfonated copolybenzimidazoles with varied IECs were prepared by random copolymerization of BCPOBDS-Na, DCDPE and DAB in Eaton's reagent at 140 °C for 45 min (Scheme 2). The IECs was controlled by controlling the molar ratio between BCPOBDS-Na and DCDPE. The high molecular weight homopolymer could not be prepared from BCPOBDS-Na and DAB because of its poor solubility in the reaction medium (gel-like product formed during the polymerization process).

The FT-IR spectra of the synthesized SPBIs in their sodium salt form are shown in Fig. 4. The characteristic absorption bands of imidazole rings at 3440 cm^{-1} (stretching of non-hydrogen-bonded N–H), 3220 cm^{-1} (stretching of hydrogen-bonded N–H), 1634 cm^{-1} (C=N stretching) and 1480 cm^{-1} (in-plane deformation of imidazole rings) are clearly observed, while the characteristic absorption band of carboxyl carbonyl groups of the dicarboxylic acid monomers at 1694 cm^{-1} completely disappeared. This indicates the complete formation of imidazole rings [38]. The chemical structure of the synthesized SPBIs was also confirmed by ^{1}H NMR spectra (Fig. 5). The peak assignments are in good agreement with the proposed chemical structures.

The solubility behaviors and the reduced viscosities of the synthesized SPBIs (in their sodium salt form) are summarized in Table 1. It can be seen that the solubility in aprotic organic solvents is dependent on the IECs of the SPBIs, and the higher IEC,

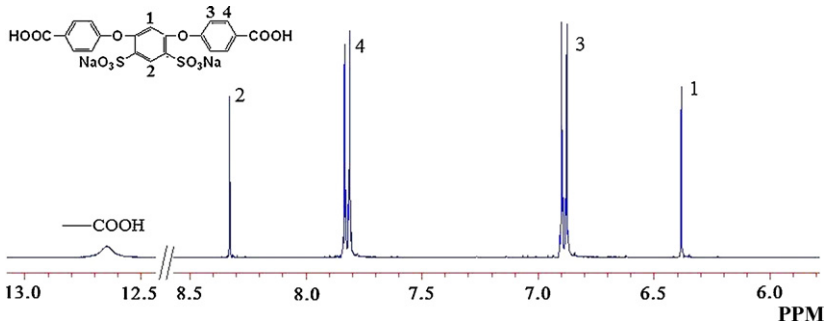

Fig. 2. ^{1}H NMR spectrum of BCPOBDS-Na in DMSO–d_6.

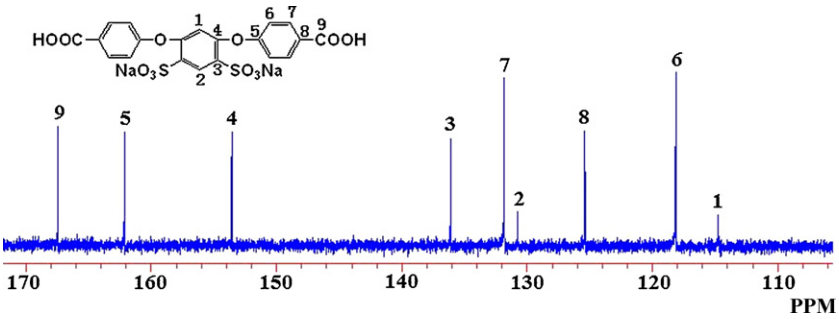

Fig. 3. ^{13}C NMR spectrum of BCPOBDS-Na in DMSO–d_6.

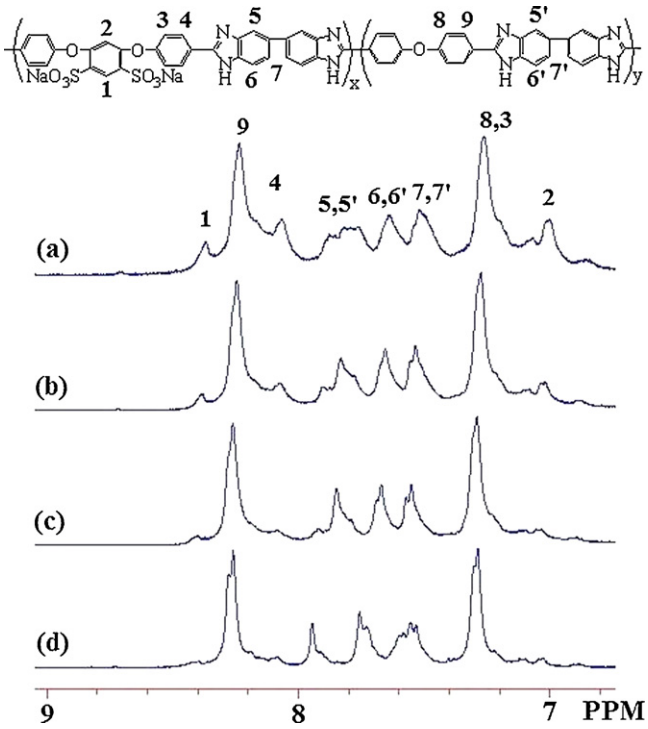

Fig. 5. ^{1}H NMR spectra of the synthesized SPBIs: (a) SPBI-11, (b) SPBI-12, (c) SPBI-13 and (d) SPBI-14).

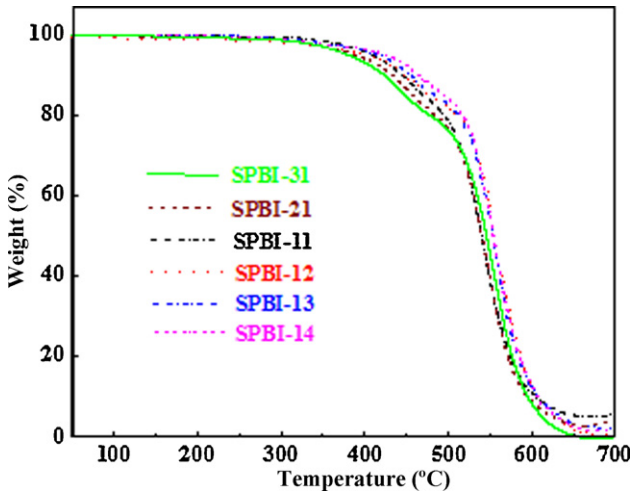

Fig. 6. TGA curves of the SPBIs (in their proton form) in air.

the poorer solubility. For example, the SPBI-31 having the highest IEC among the copolymers of this study is only partially soluble in aprotic organic solvents (DMSO, DMF, DMAc and NMP) and strong acids on heating, whereas the SPBI-14 is soluble in all the aprotic solvents and strong acids at room temperature. In addition, all the SPBIs are completely insoluble in methanol.

The reduced viscosities of the SPBIs except SPBI-31 and SPBI-21 were measured at a concentration of 0.5 g dL^{-1} in DMSO at 30 °C. As shown in Table 1, all the SPBIs displayed very high reduced viscosities (>6.5 dL g^{-1}). Moreover, transparent and tough membranes were prepared by solution cast method indicating that high molecular weight copolymers have been successfully synthesized.

3.3. Thermal stability and dynamic mechanical properties

The thermal stability of the SPBIs in their proton form was evaluated by TGA in air. Prior to measurement the samples were preheated at 150 °C for 0.5 h to remove the absorbed moisture. As shown in Fig. 6, all the samples displayed a two-stage weight loss behavior. The first stage weight loss approximately in the range of 370–480 °C is ascribed to the desulfonation reaction [24–26]. The

Table 1
Solubility and reduced viscosities (η) of the synthesized SPBIs.

Polymer	η^a (dL g^{-1})	Solubility						
		DMSO	DMF	DMAc	NMP	H_2SO_4	$MeSO_3H$	Methanol
SPBI-31	NM	+–	+–	+–	+–	+–	+–	––
SPBI-21	NM	+–	+–	+–	+–	+–	+–	––
SPBI-11	6.81	+	+–	+	+–	++	++	––
SPBI-12	8.27	++	+	+	+	++	++	––
SPBI-13	7.70	++	++	++	+	++	++	––
SPBI-14	6.56	++	++	++	+	++	++	––

Keys: "++": soluble at room temperature; "+": soluble on heating; "+–": partially soluble on heating; "––": insoluble on heating. NM: not measured because of poor solubility of the polymers in DMSO.

[a] Measured in DMSO at 0.5 g dL^{-1} and 30 °C.

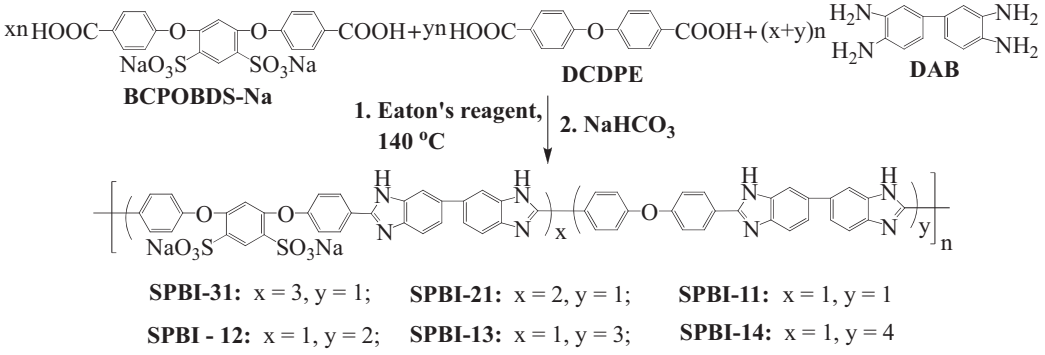

Scheme 2. Synthesis of the SPBIs.

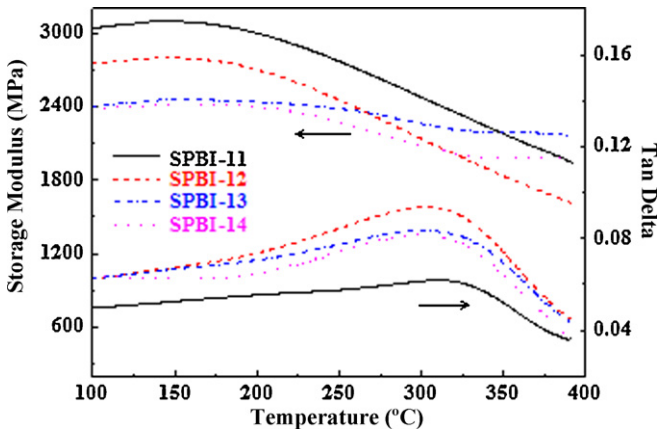

Fig. 7. DMA curves of the SPBI membranes in nitrogen.

values of weight loss in this stage are close to the theoretical values of sulfonic acid group contents in the polymers. The SPBI-11, for example, had a first stage weight loss of 14.5% which is close to the calculated value (15.3%). The decomposition temperature of the SPBIs is high enough for the applications in medium temperature (120–200 °C) fuel cells. The second-stage weight loss starting from ~480 °C is attributed to the decomposition of the polymer main chain. The TGA results indicate that the prepared SPBIs have fairly high thermal stability which well meets the requirement for use in fuel cells.

The dynamic mechanical properties of the SPBIs membranes were investigated by DMA and the curves are shown in Fig. 7. For all the membranes the storage modulus primarily increased with an increase in temperature up to ~150 °C due to the evaporation of the absorbed water which functioned as plasticizer in the membranes. The maximum storage moduli of the SPBI membranes are in the order: SPBI-11 > SPBI-12 > SPBI-13 > SPBI-14, which is just consistent with the order of IEC. The strong acid–base interactions (ionic cross-linking) restricted polymer chain movement. Higher IECs resulted in larger cross-linking densities of the membranes and therefore higher storage moduli were obtained. The glass transition temperature (T_g) was estimated from the peaks of tangent delta and the results are listed in Table 2. All the SPBIs displayed very high T_g (299–312 °C) due to ionic cross-linking as well as the rigid polymer backbones. Moreover, the SPBIs with higher IECs tend to have higher T_g due to the larger cross-linking densities.

The radical oxidative stability of the SPBIs was evaluated by the remaining weight after they were soaked in Fenton's reagent (3% H_2O_2 containing 3 ppm $FeSO_4$) at 80 °C for 12 h and the results are listed in Table 2. The SPBI-12, SPBI-13 and SPBI-14 showed more than 80% remaining weight after the Fenton's test. The SPBI-11 membrane showed significantly lower remaining weight (58%) than the others but could still keep membrane form. It should be noted that common sulfonated hydrocarbon polymers have been reported to completely dissolve in the Fenton's reagent in a very short period of time (a few hours) at the same temperature [6,8,16]. The results of the Fenton's test in this study indicate that the synthesized SPBIs have excellent radical oxidative stability.

Table 2
Ion exchange capacities (IECs), glass transition temperature (T_g), maximum storage moduli (E's) and remaining weight (RW) after Fenton's test of the SPI membranes.

Polymer	IEC (mequiv g^{-1})		T_g (°C)	E' (MPa)	RW[a] (%)
	Theoretical	Measured[b]			
SPBI-11	1.90	1.62	312	3100	58
SPBI-12	1.37	1.07	303	2800	84
SPBI-13	1.08	0.91	301	2500	85
SPBI-14	0.89	0.76	299	2400	86

[a] Measured by soaking the membranes in Fenton's reagent (3% H_2O_2 containing 3 ppm $FeSO_4$) at 80 °C for 12 h.
[b] By titration method.

3.4. PA doping, tensile properties and proton conductivity

The PA doping was performed by immersing the SPBI membranes (acid form) in 85% PA solution at 50 °C for four days and the PA uptake results are listed in Table 3. The SPBI membranes showed PA uptake in the range of 180–240% (w/w) corresponding to the doping levels φ (defined as the number of PA molecules per repeat unit) of 8.3–13. The PA uptake is also related to the IECs and the membranes with higher IECs tend to have higher PA uptake as has been observed with the sulfonated poly(2,5-benzimidazole) (ABPBI) [27].

The tensile properties of the SPBI membranes with and without PA-doping were measured and the results are listed in Table 3. It can be seen that after PA-doping the SPBI membranes showed largely decreased stress at break but greatly increased elongation at break due to the plasticization effect of PA. It is well known that the mechanical strength of PA-doped polybenzimidazole membranes is mainly dependent on the PA uptake (doping level) and the higher PA uptake, the lower mechanical strength. Polymer molecular weight is another factor which affects the mechanical strength. At the same doping level, the high molecular weight (105.1 kDa) PBI has been reported to have higher mechanical strength than the lower molecular weight (38.4 kDa) PBI [37]. In this study, the undoped SPBI-11, SPBI-12, SPBI-13 and SPBI-14 membranes showed close stress at break (89–96 MPa). Since they are structurally similar to each other, these SPBIs might have similar molecular weights. However, the PA-doped SPBI-11, SPBI-12 and SPBI-13 displayed even higher stress at break than SPBI-14 despite the larger PA uptake values of the former. The SPBI-11 membrane having the highest PA uptake (240%, w/w) displayed the largest stress at break (20 MPa). This is likely related to the differences in ionic cross-linking density of the SPBI membranes. Because sulfonic acid is more acidic than phosphoric acid the sulfonic acid groups of the SPBIs should preferentially react with the basic benzimidazole groups to form ionic cross-linking. The SPBI

Table 3
Phosphoric acid (PA) uptake, maximum stress (MS), elongation at break (EB) and proton conductivity (σ) of PA-doped membrane at 170 °C at 0% relative humidity.

Membrane	PA uptake (%w/w)	φ	MS[a] (MPa)	EB[a] (%)	σ (mS cm^{-1})	Ref.
SPBI-11	240	13	96(20)	17(92)	37.3	This study
SPBI-12	220	11	96(15)	12(144)	18.8	This study
SPBI-13	190	9.1	93(17)	22(129)	10.7	This study
SPBI-14	180	8.1	89(13)	29(90)	3.63	This study
PBI	190–210	6.0–6.6	(13–14)	(–)	18–22	37
CrL-PBI	–	8.5	(21–23)	(20–28)	–	32

–, not available from the literature.
[a] Measured at room temperature and 40% relative humidity. The data in parentheses refer to the phosphoric acid-doped membranes.

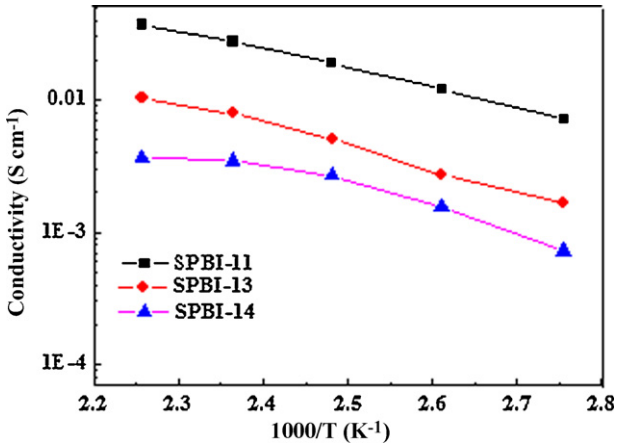

Fig. 8. Variation of proton conductivity of the SPBI membranes as a function of temperature at 0% relative humidity in cooling run.

membranes with higher IECs have higher ionic cross-linking densities which may contribute to the improvements in mechanical strength of the PA-doped SPBI membranes. It should be noted that the values of stress at break of the PA-doped SPBI membranes except SPBI-14 were comparable or higher than that of the PA-doped high molecular weight PBI membrane with similar PA uptake [37]. The PA-doped SPBI-11 membrane displayed comparable tensile strength and significantly larger elongation at break than the cross-linked commercial PBI membrane [32] despite the higher PA doping level.

The proton conductivities of the PA-doped SPBI membranes were measured at 0% relative humidity and different temperatures (90–170 °C) and the results are shown in Fig. 8. It can be seen that for all the SPBI membranes the proton conductivity increased with increasing temperature. Moreover, the membranes with higher PA-doping levels tend to have higher proton conductivities in the whole temperature range. The SPBI-11 membrane showed the highest proton conductivity (37.3 mS cm^{-1} at 170 °C) due to the highest doping level.

To check if there was any hysteresis of the proton conductivities, we measured the proton conductivity in both heating run and cooling run with the same sample membranes. Fig. 9 shows the comparison of the temperature dependence of proton conductivities of SPBI-11 membrane measured first in the cooling run (from 170 to 90 °C) and subsequently in the heating run (from 90 to 170 °C). The proton conductivities at each temperature point obtained by heating run and cooling run are quite similar indicating that the hysteresis phenomenon is negligible.

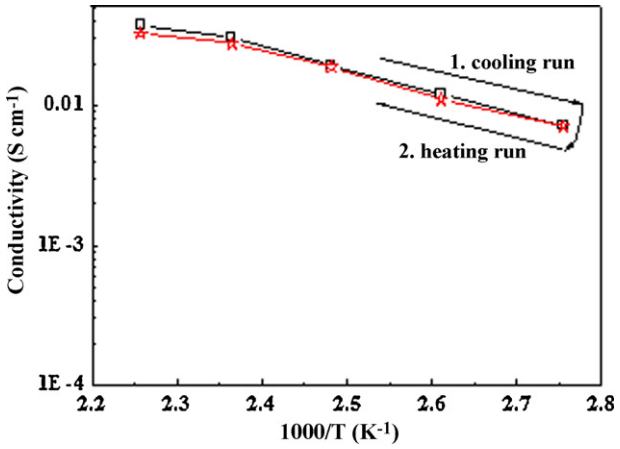

Fig. 9. Variation of proton conductivity of the SPBI-11 membranes as a function of temperature at 0% relative humidity measured first in cooling run and subsequently in heating run.

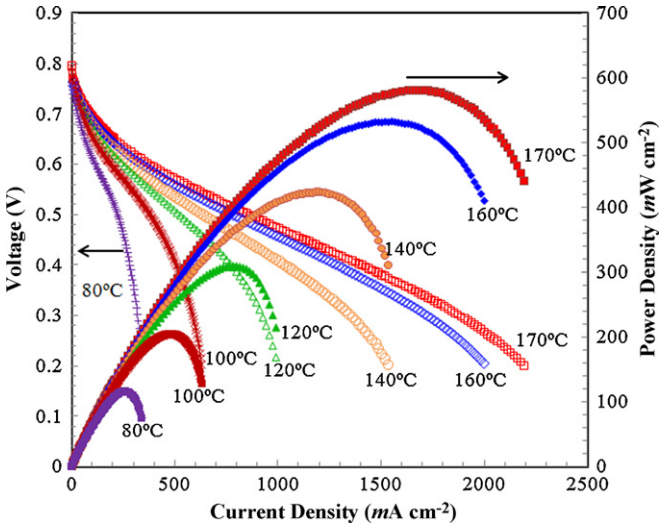

Fig. 10. Performance of the fuel cell fabricated with the PA-doped SPBI-11 membrane (PA uptake = 240%, w/w) at varied temperatures with hydrogen–oxygen gases under ambient pressure without external humidification.

3.5. Single-cell fuel cell performance

The PA-doped SPBI-11 membrane with the PA uptake of 240% (w/w) and membrane thickness of 50 μm was used as the proton exchange membrane. 40% Pt/C and PBI were used as the catalyst and binder, respectively. The Pt loading in both the anode and the cathode was 0.5 mg cm^{-2}. Preliminary fuel cell performance was evaluated with both hydrogen–oxygen and hydrogen–air gases under ambient pressure without external humidification. Fig. 10 shows the variation of fuel cell performance as a function of temperature with hydrogen–oxygen gases. It can be seen that with an increase in temperature the maximum output power density of the fuel cell increased. This is consistent with the temperature dependence of proton conductivity as shown in Fig. 8. The fast electrochemical reaction kinetics is another factor responsible for the improved fuel cell performance at elevated temperatures. The highest output power density of 0.58 W cm^{-2} was obtained at the current density of 1.68 A cm^{-2} at 170 °C with hydrogen–oxygen gases indicating good performance of the fuel cell. The fuel cell performance became significantly lower with hydrogen–air gases. Fig. 11 shows the fuel cell performance with hydrogen–air gases at 170 °C. For comparison purpose the fuel cell performance with hydrogen–oxygen gases at 170 °C is also shown in this figure. The OCV is 0.75 V and the maximum output power density is 0.32 W cm^{-2} (at the current density of 1.0 A cm^{-2}) with hydrogen–air gases which are significantly lower than those (0.80 V and 0.58 W cm^{-2}) with hydrogen–oxygen gases. This is a common phenomenon which has been observed with all the PEMFCs. It should be noted that the fuel cell performance in this study is comparable or significantly higher than those using other PA-doped polybenzimidazole membranes as the proton exchange membranes at similar Pt-loading level as reported in the literature (maximum output power densities: 0.6 W cm^{-2} at 180 °C with 1.0 mg cm^{-2} Pt loading [25], 0.28 W cm^{-2} at 160 °C with 0.5 mg cm^{-2} Pt loading [33], 0.6 W cm^{-2} at 160 °C with 1.0 mg cm^{-2} Pt loading [36], 0.32 W cm^{-2} at 125 °C with 0.5 mg cm^{-2} Pt loading [37]).

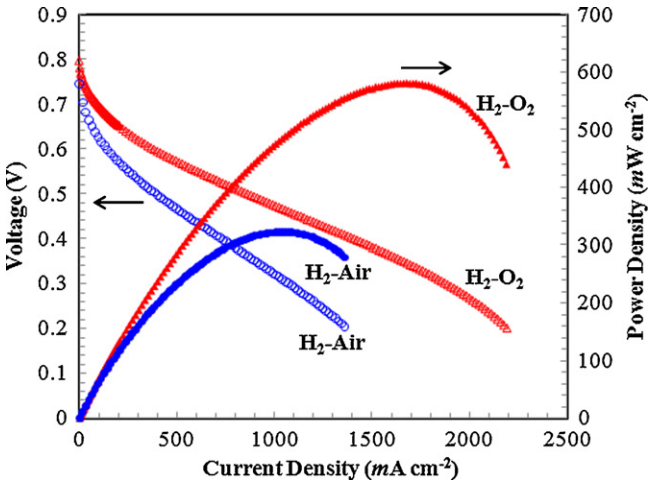

Fig. 11. A comparison of performance of the fuel cell fabricated with the PA-doped SPBI-11 membrane (PA uptake = 240%, w/w) at 170 °C with hydrogen–oxygen and hydrogen–air gases under ambient pressure without external humidification.

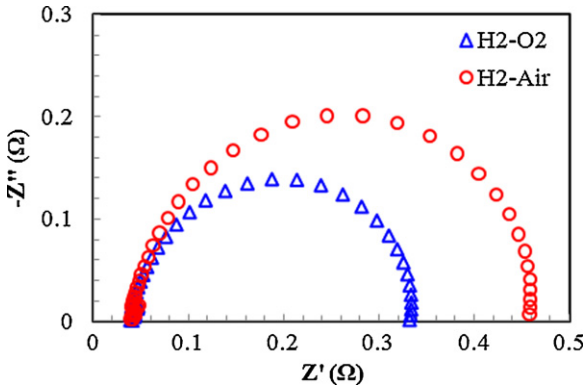

Fig. 12. EIS curves with the PA-doped SPBI-11 membrane measured at OCV at 170 °C with both hydrogen–oxygen and hydrogen–air gases under ambient pressure without external humidification.

Fig. 12 shows the EIS curves with the PA-doped SPBI-11 membrane measured at OCV at 170 °C with both hydrogen–oxygen and hydrogen–air gases under ambient pressure without external humidification. It can be seen that in each case the membrane resistance is the same (0.035 Ω), whereas the reaction resistance at electrode/electrolyte interfaces with hydrogen–oxygen gases (0.34 Ω) is lower than that with hydrogen–air gases (0.46 Ω). The lower reaction resistance with hydrogen–oxygen gases is due to the higher oxygen pressure (pure oxygen vs. air). Further studies on fuel cell performance and life-time are in progress.

4. Conclusions

(1) A new sulfonated dicarboxylic acid monomer BCPOBDS-Na has been successfully synthesized via three-step reactions and a series of high molecular weight SPBIs with varied IECs have been prepared by random copolymerization of BCPOBDS-Na, DCDPE and DAB in Eaton's reagent at 140 °C.
(2) The prepared SPBIs except the SPBI-31 and SPBI-21 showed good solubility in some aprotic solvents such as DMSO and DMAc.
(3) The SPBI membranes showed moderate PA uptake (180–240%, w/w) in 85 wt% PA solution at 50 °C and the membranes with higher IECs tended to have larger PA uptake.
(4) Ionic cross-linking is favorable for improving the mechanical strength of the PA-doped SPBI membranes. The PA-doped SPBI-11 membrane displayed the highest mechanical strength despite its highest PA uptake.
(5) High proton conductivity up to 37.3 mS cm^{-1} was achieved with the PA-doped SPBI-11 membrane at 170 °C at 0% relative humidity.
(6) The fuel cell fabricated with the PA-doped SPBI-11 membrane displayed good performance at high temperatures with hydrogen–oxygen gases under ambient pressure without external humidification, and the highest output power density of 0.58 W cm^{-2} was obtained at 170 °C.

Acknowledgments

This work was supported by National Natural Science Foundation of China (Grant No. 20474037 and 50973062), Shanghai Municipal Natural Science Foundation (Grant No. 08ZR1410300) and Chenxing Young Scholars Award Program of Shanghai Jiao Tong University. Dr. Liang Fang acknowledges China Postdoctoral Science Foundation (Grant No. 20090450696) and Shanghai Postdoctoral Scientific Program, China (Grant No. 09R21414200).

References

[1] Savadogo, J. New Mater. Electrochem. Syst. 1 (1998) 47–66.
[2] M. Rikukawa, K. Sanui, Prog. Polym. Sci. 25 (2000) 1463–1502.
[3] J. Kerres, W. Cui, S. Reichle, J. Polym. Sci. Part A: Polym. Chem. 34 (1996) 2421–2438.
[4] W. Feng, M. Hickner, Y.-S. Kim, T.A. Zawodzinski, J.E. McGrath, J. Membr. Sci. 197 (2002) 231–242.
[5] M. Schuster, K.-D. Kreuer, H.T. Andersen, J. Maier, Macromolecules 40 (2007) 598–607.
[6] K. Nakabayashi, T. Higashihara, M. Ueda, Macromolecules 43 (2010) 5756–5761.
[7] T. Kobayashi, M. Rikukawa, K. Sanui, N. Ogata, Solid State Ionics 106 (1998) 219–225.
[8] P. Xing, G.P. Robertson, M.D. Guiver, S. Mikhailenko, S. Kaliaguine, Macromolecules 37 (2004) 7960–7967.
[9] S.D. Mikhailenko, G.P. Robertson, M.D. Guiver, S. Kaliaguine, J. Membr. Sci. 285 (2006) 306–316.
[10] X. Li, C. Liu, H. Lu, C. Zhao, Z. Wang, W. Xing, H. Na, J. Membr. Sci. 255 (2005) 149–155.
[11] H. Ghassemi, J.E. McGrath, Polymer 45 (2004) 5847–5854.
[12] S. Wu, Z. Qiu, S. Zhang, X. Yang, F. Yang, Z. Li, Polymer 47 (2006) 6993–7000.
[13] C. Genies, R. Mercier, B. Sillion, N. Cornet, G. Gebel, M. Pineri, Polymer 42 (2001) 359–373.
[14] J.H. Fang, X.X. Guo, S. Harada, T. Watari, K. Tanaka, H. Kita, K. Okamoto, Macromolecules 35 (2002) 9022–9028.
[15] Y. Yin, J. Fang, T. Watari, K. Tanaka, H. Kita, K. Okamoto, J. Mater. Chem. 14 (2004) 1062–1070.
[16] J. Saito, K. Miyatake, M. Watanabe, Macromolecules 41 (2008) 2415–2420.
[17] X. Glipa, M.E. Haddad, D.J. Jones, J. Roziere, Solid State Ionics 97 (1997) 323–331.
[18] J.M. Bae, I. Honma, M. Murata, T. Yamamoto, M. Rikukawa, N. Ogata, Solid State Ionics 147 (2002) 189–194.
[19] J.A. Asensio, S. Borros, P. Gomez-Romero, J. Polym. Sci. Part A: Polym. Chem. 40 (2002) 3703–3710.
[20] S. Qing, W. Huang, D. Yan, Eur. Polym. J. 41 (2005) 1589–1595.
[21] J.A. Asensio, S. Borros, P. Gomez-Romero, Electrochim. Acta 49 (2004) 4461–4466.
[22] M.J. Ariza, D.J. Jones, J. Roziere, Desalination 147 (2002) 183–189.
[23] P. Staiti, F. Lufrano, A.S. Arico, E. Passalacqua, V. Antonucci, J. Membr. Sci. 188 (2001) 71–78.
[24] J. Jouanneau, R. Mercier, L. Gonon, G. Gebel, Macromolecules 40 (2007) 983–990.
[25] J.A. Mader, B.C. Benicewicz, Macromolecules 43 (2010) 6706–6715.
[26] H. Xu, K. Chen, X. Guo, J. Fang, J. Yin, Polymer 48 (2007) 5556.
[27] J.A. Asensio, P. Gomez-Romero, Fuel Cells 5 (2005) 336–343.
[28] J.S. Wainright, J.-T. Wang, D. Weng, R.F. Savinell, M. Litt, J. Electrochem. Soc. 142 (1995) L121–L123.
[29] Q. Li, R. He, J.O. Jensen, N.J. Bjerrum, Fuel Cells 4 (2004) 147–159.
[30] S. Yu, L. Xiao, B.C. Benicewicz, Fuel Cells 8 (2008) 165–174.
[31] L. Xiao, H. Zhang, E. Scanlon, L.S. Ramananthan, E.-W. Choe, D. Rogers, T. Apple, B.C. Benicewicz, Chem. Mater. 17 (2005) 5238–5333.
[32] Q. Li, C. Pan, J.O. Jensen, P. Noye, N.J. Bjerrum, Chem. Mater. 19 (2007) 350–352.
[33] H.L. Lin, Y.S. Hsieh, C.W. Chiu, T.L. Yu, L.C. Chen, J. Power Sources 193 (2009) 170–174.

[34] T.-H. Kim, S.-K. Kim, T.-W. Lim, J.-C. Lee, J. Membr. Sci. 323 (2008) 362–370.
[35] A. Carollo, E. Quartarone, C. Tomasi, P. Mustarelli, F. Belotti, A. Magistris, F. Maestroni, M. Parachini, L. Garlaschelli, P.P. Righetti, J. Power Sources 160 (2006) 175–180.
[36] L. Xiao, H. Zhang, T. Jana, E. Scanlon, R. Chen, E.-W. Choe, L.S. Ramanathan, S. Yu, B.C. Benicewicz, Fuel Cells 5 (2005) 287–295.
[37] J. Lobato, P. Canizares, M.A. Rodrigo, J.J. Linares, J.A. Aguilar, J. Membr. Sci. 306 (2007) 47–55.
[38] R. Bouchet, E. Siebert, Solid State Ionics 118 (1999) 287–299.